Influence of Acid Treatment on the Functional Characteristics of PtCu/C Electrocatalysts

Angelina Pavlets, Anastasia Alekseenko, and Alexey Nikulin

Abstract Two-component catalysts based on Pt-M bimetallic nanoparticles distributed on carbon support are very promising for use in low-temperature fuel cells with a proton-exchange membrane (PEM FC). At the first stage, it is necessary to obtain materials with high activity toward ORR and increased stability in stress test to use PtCu/C catalysts in PEM FC. At the second stage, it is necessary to carry out additional acid treatment of the catalysts in order to remove copper from the surface layer to minimize its selective dissolution, because it is known that Cu^{2+} cations can contaminate the polymer membrane, reducing its proton conductivity. In this work, we determined the structural parameters and composition, and also studied the electrochemical behavior of PtCu/C catalysts containing nanoparticles with a "gradient" structure in the initial state (as obtained) and after pretreatment in solutions of acid. Comparative determination of the activity of the catalysts showed that the pretreatment PtCu/C materials, which have a significantly higher stability compared to Pt/C, are not inferior to the latter in terms of their activity in the oxygen electroreduction reaction.

Keywords Pt/c · Electrocatalysts · Nanoparticles (NPs) · PtCu/C · Stability · Durability · Fuel cell (PEM FC) · Active surface area (ESA) · ORR

1 Introduction

The modern scientific community is actively developing clean and efficient energy conversion systems. The search for new resources in alternative energy has become necessary due to the serious energy crisis, as well as global environmental pollution, which have arisen in the result of excessive consumption of fossil fuels [1]. A low-temperature fuel cell with a proton exchange membrane is a promising device for converting the energy of chemical bonds into electric current with high efficiency [2].

A. Pavlets (✉) · A. Alekseenko · A. Nikulin
Chemistry Department, Southern Federal University, Rostov-on-Don, Russia
e-mail: angelina.pavlez@mail.ru

I. A. Parinov et al. (eds.), *Physics and Mechanics of New Materials and Their Applications*, Springer Proceedings in Materials 10,
https://doi.org/10.1007/978-3-030-76481-4_3

Composite materials based on platinum nanoparticles (NPs) are used as catalysts for PEM FC. It is known that Pt/C electrocatalysts are highly active in current-forming reactions such as the oxygen reduction reaction (ORR) [2, 3]. However, the widespread application of Pt catalysts is limited by the high price of the noble metal, low functional characteristics, and relatively low stability of such materials during operation [3].

To improve the functional characteristics of electrocatalysts, platinum is doped with less noble metals, such as copper, cobalt, nickel, iron, silver [4, 5]. There are numerous experimental data indicating a significant increase in the activity of bimetallic catalysts in ORR in comparison with standard Pt/C catalysts [4, 5].

The positive effect of the alloying component is due to a decrease in the interatomic distance in the crystal lattice of NPs, which facilitates the adsorption of oxygen molecules during the reaction [2, 6, 7]. Nørskov et al. showed that the use of PtM/C as ORR catalysts allows one to reduce the Pt-O bond energy, which increases the activity of such materials in comparison with composites based on pure platinum [7]. Bimetallic PtCu/C have been proven as highly active and highly stable ORR catalysts [8, 9]. Such systems are convenient to development new methods of synthesis, the study of electrochemical behavior and evolution of nanoparticles [9]. Varying the composition, controlling the architecture, size, dispersion and distribution of NPs over the support surface allows one to obtain catalysts with high electrochemical characteristics [8–10]

Materials containing bimetallic nanoparticles with *d*-metal are susceptible to selective dissolution of the alloying component, which may negatively affect the operation of the polymer membrane [5]. To solve this problem, as well as to increase the promoting effect of a less noble metal, an approach was proposed to obtain bimetallic NPs of the core (*M*)–shell (Pt) type. This method allows not only to reduce the content of expensive platinum, but also to significantly increase the efficiency of the catalyst in current-forming reactions and to reduce the tendency of the material to degrade during operation [8, 10, 11].

More novel and interesting is the approach to obtaining *M*@Pt systems with a gradient transition from a metal core to a platinum shell [12]. Layer-by-layer growth of an enriched platinum shell and smoothing of the transition between the crystal lattice of the *d*-metal and platinum, makes it possible to obtain a thermodynamically more stable system in comparison with the structure of a solid solution and pure platinum. Unfortunately, there are a number of problems associated with the obtaining of PtCu NPs of this type: (i) the formation of a copper core (oxidation of the copper surface, amorphous structure, large NPs size); (ii) deposition of precursors at subsequent stages on the formed nuclei; (iii) obtaining systems with reduced selective dissolution of copper.

Unfortunately, it is seemed impossible to apply a plurality of platinum-copper nanoparticles with a defect-free platinum shell to the surface of a carbon support and thereby prevent selective dissolution of copper. Earlier, we found that at the initial stage of electrochemical standardization of $PtCu_x$/C catalysts, an intense selective dissolution of copper occurs, while further, during stress test, the change in the Pt:Cu ratio is much less pronounced [13]. This made it possible to conditionally divide

the presented copper in the catalysts into "weak" (quickly and easily solved) and "strongly bound" (dissolves at a low rate under the conditions of subsequent stress test). We believe that the removal of "weakly bound" copper from two-component PtCu catalysts can be carried out not only electrochemically, but also by means of pretreatment in acid solutions, which opens the way for the further use of de-alloyed PtCu catalysts in PEM FC.

We have proposed a new approach to the preparation of PtCu/C electrocatalysts with a "gradient" nanoparticle structure by a multistage synthesis method. The acid treatment of the finished electrocatalyst is an additional stage of synthesis. Note that such pretreatment of PtM catalysts in acid is considered as a vital step in their preparation by various authors [8, 11, 14–17].

We believe that a bimetallic system with a gradient distribution of components is more efficient in ORR (and MOR), more quickly standardizes upon electrochemical activation (EA), and exhibits higher activity after stress tests compared to a commercial Pt/C catalyst. At the same time, the removed part of copper during acid treatment has no effect when the material is used in the MEA, and the catalysts will also have a more constant composition even during prolonged durability test.

1.1 Research Purpose

Structural and electrochemistry characteristic of PtCu/C catalysts with de-alloyed core–shell architecture is studied.

2 Experimental Part

2.1 Preparation of PtCu/C Catalysts

The method of synthesis is a modification of the method for obtaining "gradient" nanoparticles proposed earlier by A. Alekseenko et al. [12]. The synthesis of PtCu/C electrocatalysts was carried out by sequential multistage reduction of platinum (H_2PtCl_6•$6H_2O$) and copper ($CuSO_4$•$5H_2O$) precursors in an aqueous organic medium (water–ethylene glycol). Vulcan XC-72 graphitized carbon black was used as a support. The synthesis was carried out in an alkaline medium (NaOH, pH ~ 10); sodium borohydride ($NaBH_4$) was used as a reducing agent. Thus, three materials were obtained with different loading of Pt at the first stage of the synthesis, labeled as PtCu/C-1, PtCu/C-2, PtCu/C-3.

Then, the acid treatment of the obtained catalysts with 1 M nitric acid was carried out for 3 h with stirring, as a result of which three samples of PtCu/C-*n*-AC (where $n = 1, 2, 3$) were obtained.

2.2 Characterization of the Catalysts Structure

The atomic ratio of Pt: Cu metals in PtCu/C was determined by the X-ray fluorescence analysis (XRFlA) on a spectrometer with total external reflection of the X-ray radiation RFS-001 (Scientific Research Institute of Physics, Southern Federal University, Rostov-on-Don). Sample exposure time is 300 s. Registration and processing of the X-ray fluorescence spectra was carried out with the UniveRS software (Southern Federal University, Rostov-on-Don). The mass fractions of metals in the samples were determined by the gravimetric method of analysis taking into account the atomic ratio of metals.

To determine the average crystallite size, the X-ray phase analysis (XRD) was used. The X-ray diffractograms of PtCu/C materials were recorded in the angle range $2\theta = 15°–55°$ on an ARL X'TRA diffractometer (Thermo Fisher Scientific, Switzerland) using filtered CuKα radiation ($\lambda = 0.154056$ nm) at room temperature. The calculation of D_{av} was carried out for a characteristic reflection of 111 by the Scherrer formula for the most intense peak.

The microstructure of the samples was studied by transmission electron microscopy (TEM) . Photographs were taken with a JEM-2100 microscope (JEOL, Japan) at a voltage of 200 kV and a resolution of 0.2 nm.

2.3 Electrochemical Measurements

Electrochemical measurements of the catalysts were performed using an VersaSTAT 3 potentiostat in a standard three-electrode configuration at room temperature. A platinum wire was used as the counter electrode; a silver chloride electrode was used as the reference electrode. All reported potentials are relative to a reversible hydrogen electrode (RHE). A commercial catalyst was used as a standard Pt/C analog–JM20 (HiSPEC3000, Jonson Mattews, 20 wt.% Pt).

A thin film of the studied catalyst was deposited on a glassy carbon (GC) electrode to prepare the working electrode. The mixture of 900 μL of isopropanol and 100 μL of an aqueous emulsion of Nafion® 0.5% polymer was added to 6 mg of the catalyst to prepare catalytic ink. The suspension was thoroughly mixed and dispersed with ultrasound. The catalyst ink of 6 μl was then quantitatively put on the rotating disk electrode (RDE) by using a micropipette and dried in air atmosphere.

Electrochemical measurements were carried out in 0.1 M HClO4 in Ar (CV) and O_2 (LSV) atmospheres. Before electrochemical measuring each catalyst was electrochemically activated by 100 potential cycles in the potential range of 0.04–1.2 V at a scan rate of 200 mV/s. Then, two cycles were recorded with a scan rate of 20 mV/s in the potential range of 0.04–1.2 V to determine the electrochemically active surface area (ESA) . The ESA of catalyst was calculated by integrating the area in the hydrogen underpotential deposition (HUPD) region, taking into account

that the average charge density spent on the formation of one monolayer hydrogen atom on a polycrystalline of Pt electrode is 210 $\mu C/cm^2$.

The oxygen reduction reaction activity of the samples was evaluated by performing linear sweep voltammetry (LSV) in the potential range 0.1–1.2 V at a scan rate of 20 mV/s under a certain rotating speed (400, 900, 1600, 2500 rpm). The kinetic current at 0.9 V was calculated by using the Koutetsky–Levich equation: $1/j = 1/j_k + 1/j_d$, where j is the experimentally measured current, j_d is the diffusion current, and j_k is the kinetic current.

The durability test was investigated by repeated CV scanning cycles up to 5000 cycles between 0.6 V and 1.0 V at a sweep rate of 100 mV/s [17]. After 1000, 3000 and 5000 CV ESA was measured by the above method. The catalytic activity of the electrodes after the durability test was also studied and compared.

3 Results and Discussion

Initially, in the course of the study, a number of PtCu/C materials were obtained with a close mass fraction of Pt from 22.0 to 24.3 wt. % (Table 1). The obtained samples are characterized by a close atomic ratio of metals from $PtCu_{0.67}$ to $PtCu_{0.79}$ (Table 1). After acid treatment, the copper content in all samples is reduced by almost two times (Table 1).

All of PtCu/C samples are characterized by a small average crystallite size (less than 3 nm), which is calculated using the Scherrer equation (Table 1). A graphitized carbon peak (200) of $2\theta = 25$ is identified on diffractograms (Fig. 1). The most intense peak of the face (111) is shifted towards large angles of 2θ, which is a consequence of the alloying of Pt and Cu. Another evidence of alloying the components is the absence of peaks of the pure Pt and Cu. The fact that the peak of the face (111) is between the peaks of pure platinum and copper may be related to the effect of lattice deformation of the platinum shell caused by the Cu or Pt-Cu core [6].

Table 1 Structural characteristics of obtained PtCu/C electrocatalysts

Sample	Metals loading, wt. %	Pt loading, wt. %	Average crystallite size, nm (XRD)	Position of (111) maximum, 2θ, degrees	Composition
PtCu/C-1	27.9	22.2	2.7	41.3	$PtCu_{0.79}$
PtCu/C-1-AC	24.1	21.4	2.7	40.8	$PtCu_{0.39}$
PtCu/C-2	27.0	22.0	2.5	41.2	$PtCu_{0.70}$
PtCu/C-2-AC	23.2	20.9	2.7	41.0	$PtCu_{0.34}$
PtCu/C-3	29.6	24.3	2.7	41.4	$PtCu_{0.67}$
PtCu/C-3-AC	24.8	22.2	2.9	40.8	$PtCu_{0.36}$

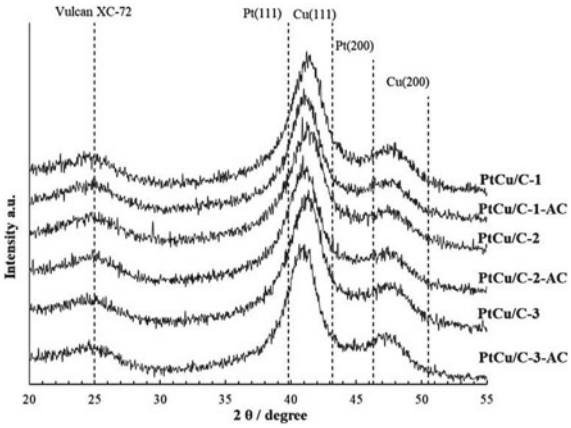

Fig. 1 XRD patterns of obtained PtCu/C materials

As expected, after forced leaching of copper, the peak of the face (111) shifts towards smaller angles of 2θ, which is due to the lower copper content in the PtCu/C-*n*-AC samples compared to PtCu/C-*n* (Fig. 1, Table 1). Also, in all XRD patterns, the peaks corresponding to CuO and Cu_2O are not identified, however, their absolute absence cannot be ruled out, since copper oxides can be in an amorphous state.

Transmission electron microscopy was performed on one of the PtCu/C samples and its corresponding acid-treated analog (Fig. 2). The initial catalyst is characterized by the presence of particles with a core–shell structure of small size of about 5 nm (Fig. 2a), which indicates the success of the applied synthesis method. After acid treatment, this structure is also retained, which may indicate leaching only of the surface copper (Fig. 2b). It is also worth noting that, after acid treatment, the presence of homogeneous nanoparticles of small size (no more than 2–3 nm) is observed in the sample; apparently, of pure Pt.

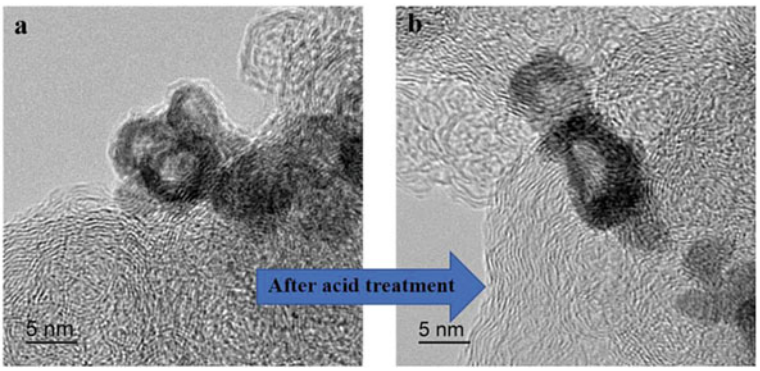

Fig. 2 TEM of the one of PtCu/C electrocatalysts before (**a**) and after (**b**) acid treatment

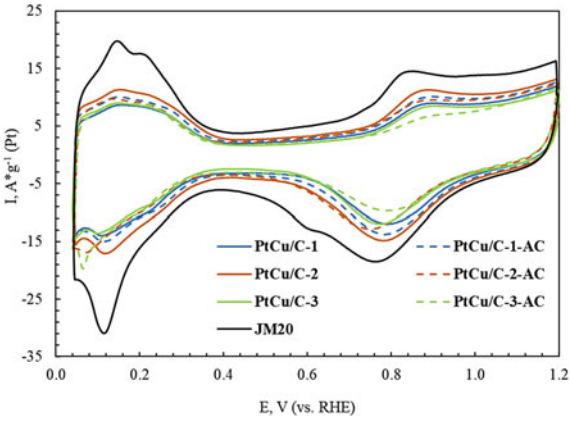

Fig. 3 Cyclic voltammograms of commercial Pt/C and PtCu/C electrodes after electrochemical activation, 0.1 M $HClO_4$, Ar atmosphere, scan rate is 20 $mV \cdot s^{-1}$

Figure 3 shows the cyclic voltammograms of the native and acid-treated PtCu/C samples, as well as the commercial Pt/C analog after electrochemical activation. The CV type is typical for Pt-polycrystalline electrode. Voltammograms show areas of hydrogen underpotential deposition (HUPD) between 0.05 and 0.4 V, as well as areas of formation and reduction of Pt-O in the range of 0.7–1.0 V. For PtCu/C samples, there are no features of Cu bulk dissolution (Fig. 3), which may indicate both the absence of copper on the nanoparticles surface and the possible chemical dissolution of Cu. With a cathodic sweep in the range of 0.7–1.2 V, all bimetallic catalysts (except for PtCu/C-2-AC) exhibit lower overpotential on the oxide reduction than the commercial analogue JM20 [15].

ESA determined by hydrogen adsorption/desorption on CV are close for PtCu/C and range from 41 to 52 m^2g^{-1} (Pt) (Table 2). It should be noted that acid treatment did not have a clear effect on the active surface area. Thus, for the PtCu/C-1-AC sample, ESA increases in comparison with the native sample, while the PtCu/C-2-AC sample loses 11 m^2g^{-1} (Pt) (Table 2). In this regard, it can be assumed that

Table 2 Electrochemical characteristics and composition of the PtCu/C and Pt/C electrocatalysts after electrochemical activation (EA)

Sample	Composition after EA	ESA, $A \cdot g^{-1}$ (Pt)	I_k, mA	I_{mass}, $A \cdot g^{-1}$ (Pt)	I_{sp}, $A \cdot m^{-2}$ (Pt)	Number of $\bar{e}$	$E_{1/2}$, V
PtCu/C-1	$PtCu_{0.32}$	43 ± 4	1.92	255	5.4	3.8	0.92
PtCu/C-1-AC	$PtCu_{0.26}$	50 ± 5	1.75	222	4.4	4.1	0.92
PtCu/C-2	$PtCu_{0.23}$	52 ± 5	2.50	317	8.9	4.1	0.93
PtCu/C-2-AC	$PtCu_{0.24}$	41 ± 4	1.66	222	5.4	4.4	0.91
PtCu/C-3	$PtCu_{0.26}$	52 ± 5	3.23	381	7.4	3.9	0.93
PtCu/C-3-AC	$PtCu_{0.27}$	48 ± 5	2.62	332	7.0	3.8	0.92
JM20	–	80 ± 8	1.37	180	2.2	3.8	0.92

during the chemical and electrochemical treatment of catalysts, the formation of super-porous structures does not occur for the Pt-Cu obtained systems [16].

Based on Table 2, the samples are characterized by close values of the metal ratio after electrochemical measurements. The advantage of acid treatment of PtCu/C electrocatalysts appears to be observed. For example, during the electrochemical activation, the copper content in the PtCu/C-2 sample decreases by a factor of 3, while for the PtCu/C-2-AC sample, this value is 1.4 times. Thus, during the preliminary acid treatment, the catalyst surface is standardized due to the dissolution of the alloying component unprotected by the platinum shell. It is also possible to estimate what amount of copper dissolves during the reorganization of the NPs surface during potential cycling. In general, the obtained results indicate a fairly high stability of the pretreated Pt-Cu nanoparticles.

Figure 4a shows the ORR polarization curves with potentials of the ORR onset (inset in Fig. 4a). As seen from Fig. 4a, the ORR curve of a commercial catalyst is shifted to lower potentials. Despite the fact that the surface area of the commercial Pt/C catalyst is still higher than for the PtCu/C samples, the latter are characterized by a higher activity in the oxygen reduction reaction (Table 2). So, according to the mass activity, the initial samples can be arranged in a row: PtCu/C-3 > PtCu/C-2 > PtCu/C-1 > JM20. The same situation is observed for acid-treated materials: PtCu/C-3-AC > PtCu/C-2-AC = PtCu/C-1 > JM20 (Table 2). According to the potential of the ORR onset, all electrocatalysts can be arranged as follows: PtCu/C-2 > PtCu/C-3 > PtCu/C-1-AC > PtCu/C-3-AC > PtCu/C-1 > PtCu/C-2-AC = JM20 (inset in Fig. 4a). As can be seen from the presented rows, bimetallic catalysts are characterized by better catalytic activity in ORR in comparison with commercial Pt/C.

Figure 4b shows straight lines in the Koutetsky–Levich coordinates. Based on the *y*-intercept coefficient of the line, it can be concluded that the PtCu/C samples are characterized by higher specific currents. High values of the correlation coefficients indicate the correctness and high accuracy of the measurements (Fig. 4b). Moreover, based on the equations of straight lines, the determined number of electrons in the reaction is close to 4 (Table 2), which indicates the minimum occurrence of side reactions.

After acid treatment, the mass and specific activity of PtCu/C-*n*-AC materials slightly decreases compared to the starting PtCu/C-*n* materials, but still remains higher than for the commercial analogue.

The stability of PtCu/C-1, PtCu/C-2, as well as their acid-treated analogs and commercial Pt/C, was evaluated by long-term stress test for 5000 voltampere cycles. The choice of these materials is due to the fact that the native PtCu/C samples are characterized by different mass activities, and their acid-treated analogs are similar in parameters.

The composition of the catalysts after the durability test changed insignificantly (Tables 2 and 3), which confirms the stability of the composition of bimetallic NPs. As can be seen from the histogram in Fig. 5a, the PtCu/C-2-AC sample is characterized by the highest stability equal to 94%, while the lowest value for commercial Pt/C material is 78%. It can also be seen from the histogram that the degradation rate of a commercial sample is higher than for Pt-Cu materials. The residual ESA value

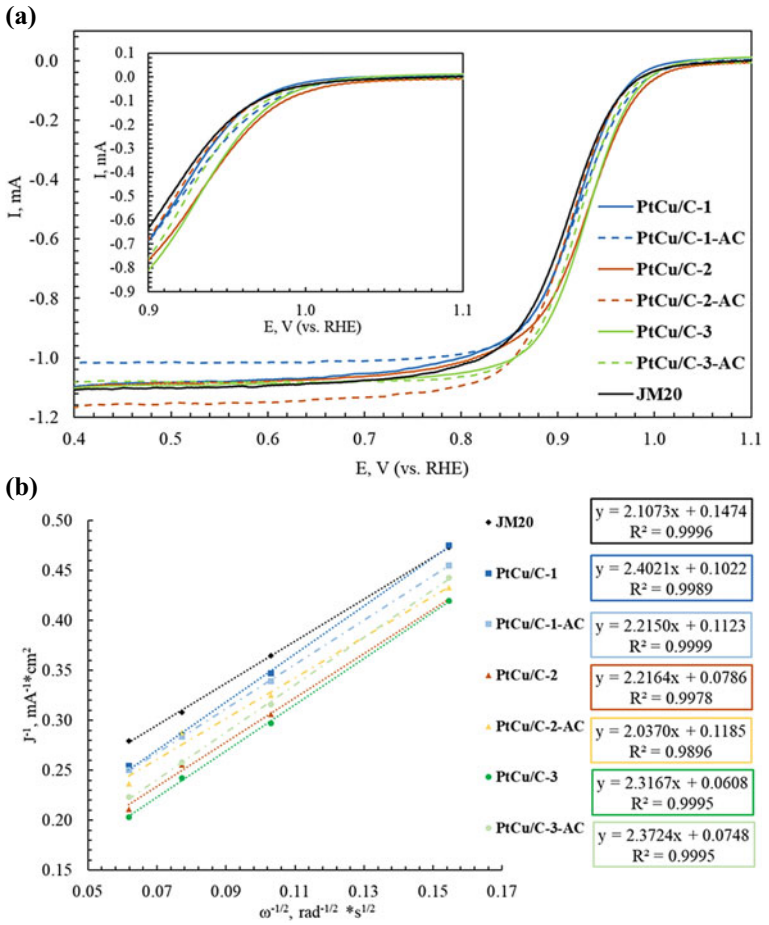

Fig. 4 **a** ORR polarization curves, 0.1 M $HClO_4$, O_2 atmosphere the rotation speed of the disk is 1600 rpm, scan rate is 20 mV·s^{-1}; **b** j^{-1}–$\omega^{-1/2}$ dependences at 0.90 V potential for obtained PtCu/C and Pt/C electrodes

Table 3 Electrochemical characteristics and composition of the PtCu/C and Pt/C electrocatalysts after stress test

Sample	Composition	ESA, A·g^{-1} (Pt)	I_{mass}, A·g^{-1} (Pt)	I_{sp}, A·m^{-2} (Pt)	Number of ē	$E_{1/2}$, V
PtCu/C-1	$PtCu_{0.29}$	37	300	8.0	3.9	0.92
PtCu/C-1-AC	$PtCu_{0.25}$	42	311	7.4	4.1	0.92
PtCu/C-2	$PtCu_{0.22}$	45	210	6.2	4.0	0.92
PtCu/C-2-AC	$PtCu_{0.21}$	45	340	9.4	4.4	0.91
JM20	–	62	59	1.0	4.1	0.89

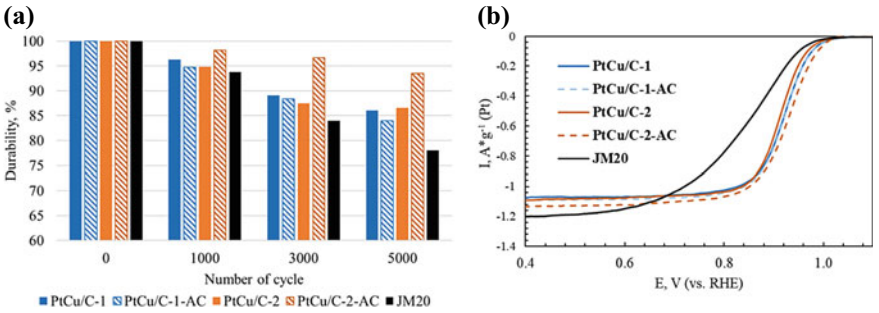

Fig. 5 **a** Relative ESA change during durability test and **b** ORR polarization curves of PtCu/C and Pt/C samples after durability test, 0.1 M $HClO_4$, O_2 atmosphere the rotation speed of the disk is 1600 rpm, scan rate is 20 $mV \cdot s^{-1}$

after stress test is the highest for PtCu/C-2 and PtCu/C-2-AC materials among all of obtained catalysts (Table 3). It should be noted that the PtCu/C-2-AC sample is characterized by the highest catalytic activity after the durability test: its mass activity exceeds that for the commercial one by 5.8 times, and the specific activity is 9.4 times higher (Table 3).

Figure 5b shows the polarization curves of the investigated materials after the durability test. The commercial analogue JM20 showed the greatest changes in the diffusion-kinetic region, which also indicates a high degradation of the material.

4 Conclusion

In this study, three PtCu/C materials were obtained, which were further treated with nitric acid. Comparison of performances showed that bimetallic catalysts are characterized by a small nanoparticle size (about 5 nm), a core–shell structure, and a high catalytic activity. Acid pretreatment of PtCu/C catalysts have shown some advantages: (i) it allows one to get rid of surface copper and stabilizes the NPs composition during measurements; (ii) it increases the stability of the electrocatalyst. The first advantage is a vital condition for the further use of bimetallic catalysts in real PEM FC.

Acknowledgements This research was supported by the Russian Science Foundation (grant No. 20-79-10211).

References

1. S. Chu, A. Majumdar, Nature **488**, 294 (2012)
2. M. Debe, Nature **486**, 43 (2012)
3. Y. Nie, L. Li, Z. Wei, Chem. Soc. Rev. **44**(8), 2168 (2015)
4. N. Jung, D.Y. Chung, J. Ryu, S.J. Yoo, Y.E. Sung, Nano Today **9**(4), 433 (2014)
5. V.E. Guterman, T.A. Lastovina, S.V. Belenov, N.Y. Tabachkova, V.G. Vlasenko, I.I. Khodos, E.N. Balakshina, J. Solid State Electrochem. **18**(5), 1307 (2013)
6. P. Strasser, S. Koh, T. Anniyev, J. Greeley, K. More, C. Yu, Z. Liu, S. Kaya, D. Nordlund, H. Ogasawara, M.F. Toney, A. Nilsson, Nature Chem **2**, 454 (2010)
7. J.K. Nørskov, J. Rossmeisl, A. Logadottir, L. Lindqvist, J.R. Kitchin, T. Bligaard, H. Jónsson, J. Phys. Chem. B **108**(46), 17886 (2004)
8. J. Garcia-Cardona, I. Sirés, F. Alcaide, E. Brillas, F. Centellas, P.L. Cabot, Int. J. Hydrogen Energy **45**(10), 20582 (2020)
9. N. Hodnik, M. Bele, A. Recnik, N.Z. Logar, M. Gaberšček, S. Hočevar, Energy Procedia **29**, 208 (2012)
10. N. Hodnik, C. Jeyabharathi, J.C. Meier, A. Kostka, K.L. Phani, A. Rečnik, M. Bele, S. Hočevar, M. Gaberšček, K.J.J. Mayrhofer, Phys. Chem. Chem. Phys. **16**(27), 13610 (2014)
11. M. Oezaslan, F. Hasché, P. Strasser, J. Phys. Chem. Lett. **4**(19), 3273 (2013)
12. A.A. Alekseenko, V.E. Guterman, S.V. Belenov, V.S. Menshikov, N.Yu. Tabachkova, O.I. Safronenko, E.A. Moguchikh, Int. J. Hydrogen Energy **43**(7), 3676 (2018)
13. A.A. Alekseenko, S.V. Belenov, V.S. Men'shchikov, V.E. Guterman, Russ. J. Electrochem. **54**, 415 (2018)
14. V.R. Stamenkovic, S.B. Mun, K.J.J. Mayrhofer, Ph.N. Ross, N.M. Markovic, J. Am. Chem. Soc. **128**, 8813 (2006)
15. Y. Sohn, J.H. Park, P. Kim, J.B. Joo, Curr. Appl. Phys. **15**(9), 993 (2015)
16. D. Wang, Y. Yu, H.L. Xin, R. Hovden, P. Ercius, J.A. Mundy, H. Chen, J.H. Richard, D.A. Muller, F.J. DiSalvo, H.D. Abruña, Nano Lett. **12**(10), 5230 (2012)
17. A.A. Alekseenko, E.A. Moguchikh, O.I. Safronenko, V.E. Guterman, Int. J. Hydrogen Energy **43**(51), 22885 (2018)